NANO LETTERS
Letter
Cite This: Nano Lett. XXXX, XXX, XXX−XXX
pubs.acs.org/NanoLett

Wearable Sweat Band for Noninvasive Levodopa Monitoring

Li-Chia Tai,[†,‡,§] Tiffany S. Liaw,[†,‡,§] Yuanjing Lin,[†,‡,§,⊥] Hnin Y. Y. Nyein,[†,‡,§] Mallika Bariya,[†,‡,§] Wenbo Ji,[†,‡,§] Mark Hettick,[†,‡,§] Chunsong Zhao,[†,‡,§] Jiangqi Zhao,[†,‡,§] Lei Hou,[†,‡,§] Zhen Yuan,[†,‡,§] Zhiyong Fan,[⊥] and Ali Javey*[,†,‡,§]

[†]Department of Electrical Engineering and Computer Sciences and [‡]Berkeley Sensor and Actuator Center, University of California, Berkeley, California 94720, United States

[§]Materials Sciences Division, Lawrence Berkeley National Laboratory, Berkeley, California 94720, United States

[⊥]Department of Electronic and Computer Engineering, Hong Kong University of Science and Technology, Clear Water Bay, Kowloon, Hong Kong SAR, China

Supporting Information

ABSTRACT: Levodopa is the standard medication clinically prescribed to patients afflicted with Parkinson's disease. In particular, the monitoring and optimization of levodopa dosage are critical to mitigate the onset of undesired fluctuations in the patients' physical and emotional conditions such as speech function, motor behavior, and mood stability. The traditional approach to optimize levodopa dosage involves evaluating the subjects' motor function, which has many shortcomings due to its subjective and limited quantifiable nature. Here, we present a wearable sweat band on a nanodendritic platform that quantitatively monitors levodopa dynamics in the body. Both stationary iontophoretic induction and physical exercise are utilized as our methods of sweat extraction. The sweat band measures real-time pharmacokinetic profiles of levodopa to track the dynamic response of the drug metabolism. We demonstrated the sweat band's functionalities on multiple subjects with implications toward the systematic administering of levodopa and routine management of Parkinson's disease.

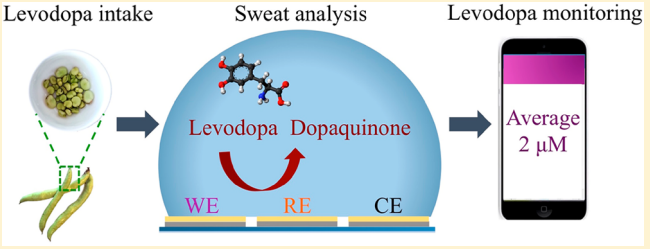

KEYWORDS: *Wearable sweat sensor, Parkinson's disease, levodopa detection, noninvasive drug monitoring, dosage optimization*

Levodopa is the medication administered to treat patients with Parkinson's disease.[1−7] Despite its success, an individual's responses to levodopa can vary due to factors such as dietary intake, age, gender, and drug administration history.[8−12] These variations can lead to unfavorable fluctuations of the subject's motor and cognitive functions if the levodopa dosage is not tailored toward the individuals.[12−14] Therefore, levodopa monitoring is an essential part of the treatment for Parkinson's disease. The gold standard for optimizing levodopa dosage involves an assessment of the motor function of a Parkinson's disease patient.[9] This method requires clinicians to evaluate the subject's motor functions, leading to difficulty of point-of-care testing and ambiguity in drug dosage. To address this challenge, monitoring blood levodopa concentration stands out as a viable solution.[15−18] However, blood-based detection is hampered by its need for invasive sampling and separate analytical tools, making it inappropriate for the long-term and frequent measurements that are necessary due to the dynamic nature of drug metabolism.

Taking this into consideration, human sweat is an alternative to blood due to its accessibility through noninvasive procedures and its abundance of biomolecules. Like other drug molecules that undergo xenobiotic metabolism pathway, levodopa excretes through sweat with its concentration in sweat exhibiting a potential correlation with that in human plasma.[19−22] Additionally, under standard levodopa dosage, sweat levodopa level shows up in the micromolar ranges,[17−19] making it amenable for reliable detection with current technologies.[23,24] For these reasons, sweat presents an ideal means for nonobstructive monitoring of levodopa for dosage optimization. Sweat sensing patches have been employed for drug tests in athletic doping control, drug abuse investigation, and forensic inspection.[25,26] Recently, sweat sensors for drugs and their related biomolecules have also been demonstrated via optical and electrochemical techniques.[27−32] In particular, the electrochemical approach represents an attractive method owing to its advantages for electronic integration, economical cost, sensitivity, and selectivity.[29−36]

In this work, we expand the strength of the electrochemical sensor through integrated surface innovations at the physical and chemical levels. The incorporation of gold dendritic nanostructures onto the electrodes remarkably enhanced the

Received: June 18, 2019
Revised: July 26, 2019
Published: August 5, 2019

DOI: 10.1021/acs.nanolett.9b02478
Nano Lett. XXXX, XXX, XXX−XXX

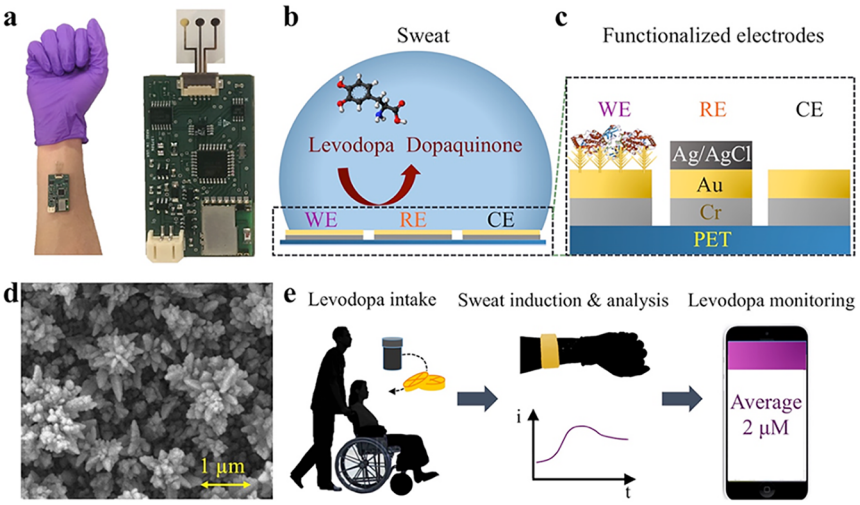

Figure 1. Schematic of the *s*-band and drug sensing mechanism. (a) Optical image of the *s*-band worn on a subject's wrist. (b) Sensing mechanism of the levodopa sensor. WE, RE, and CE are working electrode, reference electrode, and counter electrode, respectively. (c) Cross-section view of the gold electrodes on a flexible sensor patch. (d) Scanning electron microscope image of the gold dendritic structures. (e) Real-time sweat levodopa monitoring using the *s*-band after levodopa intake.

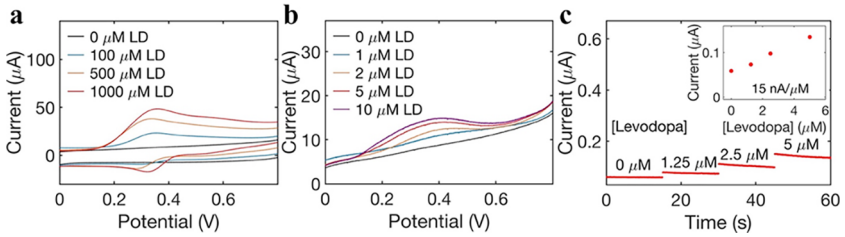

Figure 2. Characterization of the functionalized working electrode in PBS. (a) CV of levodopa (LD) dissolved in PBS and (b) zoom-in view for smaller concentration range. (c) Amperometric response of levodopa dissolved in PBS. Inset shows the calibration curve.

detection limit of the levodopa sensor down to about 1 μM in sweat solution, a couple-times improvement compared to previous work tested in human fluid.[37] Moreover, the cross-linking mechanisms with glutaraldehyde provide us chemically robust enzymatic structures to achieve sensor stability for long-term and continuous usage.[37−40] This approach effectively connects existing sensor enhancement technologies into a consolidated platform for prolonged sensor operation. Our solutions effectively address the challenges for drug detection, which are attributed to the generally low concentration of drugs in human sweat and the long time scale of drug metabolism.

The design of the wearable sensor packaged into a sweat band (*s*-band) is illustrated in Figure 1a. The sensor is fabricated on a polyethylene terephthalate (PET) substrate, and it employs a standard three-electrode configuration with a functionalized levodopa sensing electrode as working electrode, a Ag/AgCl top layer as reference electrode, and a Au top layer as counter electrode. As shown in Figure 1b, during amperometric measurement, levodopa excreted in sweat can be oxidized via tyrosinase enzyme to dopaquinone.[37] This process generates a Faradaic current that can be further calibrated into its corresponding sweat levodopa concentration. The cross-section schematic of the electrodes is shown in Figure 1c, and Figure 1d shows a scanning electron microscope image of the gold dendrites to validate the successful growth and density of the nanostructures. To achieve the enhancement on sensitivity, gold nanodendrites with largely increased surface area are synthesized via overpotential deposition approach on the evaporated Au/Cr conductive layer.[38,39] Further, thionin acetate salts are deposited via cyclic voltammetry (CV) method conformally on the as-synthesized dendritic gold structures, and glutaraldehyde/tyrosinase is drop-casted onto the working electrode. Glutaraldehyde serves as the cross-linker to immobilize the tyrosinase enzyme that facilitates the electrochemical oxidation of levodopa.[37,40] It is also worth mentioning that the dendritic gold plays a pivotal role to provide adequate interface for enzyme loading and molecular contact to achieve an improved sensing performance. The final modification step for the working electrode involves the drop-casting of Nafion, which enhances the long-term stability and antifouling features of the electrochemical sensor.[41] The prospective application of the sensor is illustrated in Figure 1e, which shows the application of iontophoresis for noninvasive and stationary stimulation of sweat to monitor levodopa levels after a subject consumes the drug. The *s*-band enables continuous monitoring of levodopa, which allows for personalized optimization of levodopa dosage.

The functionalized levodopa sensing electrode was characterized with CV scanning, which indicated the oxidation peak of levodopa. Figure 2a shows the CV curves using the functionalized electrode in phosphate-buffered saline (PBS) with different concentrations of levodopa. The oxidation and reduction peaks for levodopa are around 0.34 and 0.30 V (method of peak identification is illustrated in Figure S1), respectively, which are consistent with the literature.[23] Figure 2b shows a CV in the proximity of levodopa's oxidation peak in the physiologically relevant concentration range.[19] The

DOI: 10.1021/acs.nanolett.9b02478
Nano Lett. XXXX, XXX, XXX−XXX

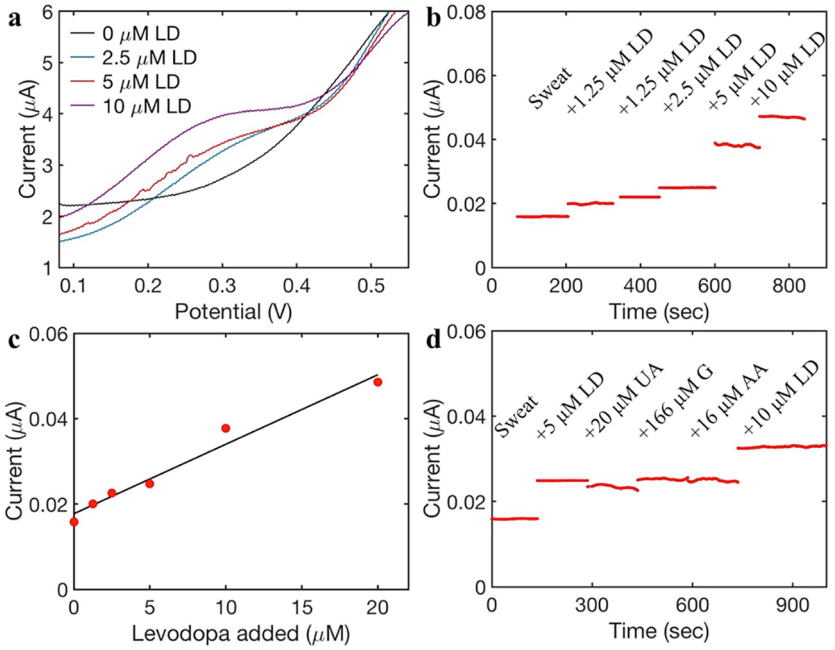

Figure 3. Characterization of the levodopa sensor in sweat solution. (a) CV of levodopa dissolved in sweat. (b) Amperometric response of levodopa dissolved in sweat and the (c) corresponding calibration curve. (d) Interference study of the levodopa sensor after the addition of levodopa (LD), uric acid (UA), glucose (G), and ascorbic acid (AA).

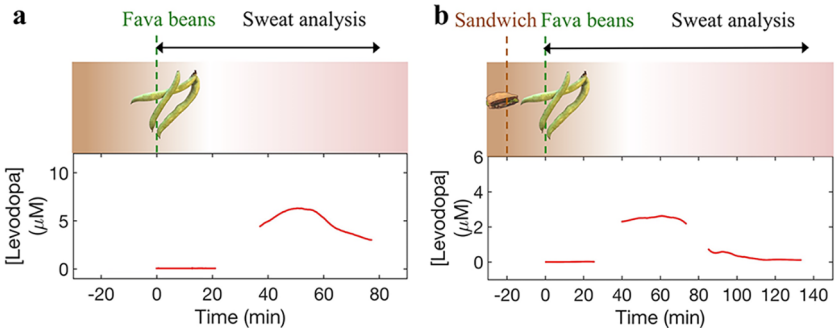

Figure 4. Levodopa monitoring via iontophoresis-induced sweat. Sweat levodopa concentration is monitored continuously after fava beans consumption and subsequent applications of iontophoresis (a) without and (b) with prior dietary consumption. The horizontal axis indicates the time elapsed after the subject consumes 450 g of fava beans.

functionalized electrode responds to levodopa with high sensitivity in the micromolar range. This is a remarkable enhancement of more than two orders of magnitude compared to the response of a bare Au electrode (Figure S2). Figure 2c shows the amperometric response of levodopa at the oxidation potential (0.34 V). The inset displays the calibration curve with a sensitivity of 15 nA/μM, which is on par with the best levodopa sensors reported.[23] This is notable considering the simplicity of electrode functionalization and the electrode's excellent stability for long-term usage.

The sensors were further characterized in sweat solution to demonstrate the *s*-band's practical applications for noninvasive monitoring. Figure 3a shows a CV in the proximity of levodopa's oxidation peak, which is identified to be 0.25 V. The amperometric response of levodopa was similarly tested at the oxidation potential, shown in Figure 3b. The corresponding calibration curve in sweat is displayed in Figure 3c, and the sensitivity is found to be 1.7 nA/μM. This value is different from that in PBS and is expected due to biofouling activity.[29] For the purpose of the study, we define drift as the maximum change in the signal of the amperometric response of a fixed concentration (e.g., 10 μM) over a period of operation (e.g., 30 min). The sensor drift is approximately 18 nA as shown in Figure S3. The error of concentration measurement due to drift is estimated to be 1.2 μM. The limit of detection is 1.25 μM as shown in Figure 3b. The signal-to-noise ratio (SNR) is the ratio of the square of the amplitude of the signal to the background noise. On the basis of Figure S3b, the amperometric response signal is found to be 225 nA. During the measurement, the noise level is observed to be approximately 50 nA, which results in a SNR of 20. The selectivity of the sensor is essential in the presence of other common sweat biomolecules. Therefore, the amperometric responses of the addition of levodopa and its potential interferents such as uric acid (20 μM), glucose (166 μM), and ascorbic acid (16 μM) are recorded in Figure 3d. The concentrations are chosen to be in their physiologically relevant ranges.[29−32] The result shows that the interference on the levodopa sensor performance is within an error range of 0.35 μM.

To explore the viability of using the *s*-band to track the metabolism of levodopa in human subjects, sweat was

DOI: 10.1021/acs.nanolett.9b02478
Nano Lett. XXXX, XXX, XXX−XXX

extracted from a healthy volunteer through iontophoresis and after *Vicia faba* (fava bean) consumption. Fava beans are levodopa-containing legumes consumed for culinary and medicinal purposes.[18] The use of fava beans allows for extensive testing of the *s*-band's functionalities on non-vulnerable, healthy subjects.

Figure 4a shows the time progression panel of fava beans consumption and iontophoresis application as well as continuous sensor readings of the sweat levodopa concentration. The result demonstrates that the *s*-band can continuously capture the sweat levodopa trend that resembles the blood levodopa profile observed.[15−18] During iontophoretic stimulation, sweating begins after iontophoresis and lasts for about 20 to 45 min. Therefore, two consecutive applications of iontophoresis are performed at −20 and 25 min, with respect to the time of fava beans intake, to cover a broad time range that captures levodopa's metabolic trend. The subjects consume 450 g of fava beans after 12 h of fasting, and their sweat levodopa concentration is monitored after each iontophoresis. The observed sweat levodopa level versus time shows an increasing trend up to 6.6 μM at about 47 min, after which the concentration begins to decrease. The levodopa concentration decreases to 3.3 μM at about 74 min, so the half-life of the decay is found to be 27 min. The time scales of levodopa's half-life and its time of peak concentration are expected based on previous observations.[15−18] In Figure 4b, the subject first consumes a 426 g sandwich (see Methods) followed by 450 g of fava beans. Three consecutive applications of iontophoresis are performed at −20, 25, and 80 min, with reference to the time of fava beans consumption. The result shows a slight delay of 13 min in the pharmacokinetic peak time compared to that in Figure 4a. This finding is expected as dietary intake can affect the pharmacokinetic profile of levodopa in human secretory systems.[11] The data in Figures 4a and b verifiy the *s*-band's capability of continuous levodopa measurement.

While sweating caused by iontophoresis can be limited in its duration, sweating generated through exercise can typically last longer and allow us to capture a more complete picture of the drug's pharmacokinetics. Figure 5 explores the possibility of exercise as a means to extend the sweating period. Figure 5a shows the time progression panel of fava beans intake and an image of a subject engaging in ergometer cycling. The representative pharmacokinetic profiles of sweat levodopa for three different subjects are included. In each trial, the subject consumes 450 g of fava beans and exercises on a stationary ergometer. Each subject exercises for multiple trials, and the cumulative result is shown in Figure 5b, with the averaged time of peak concentration for subject 1, 2, and 3 being 44 ± 20 min, 42 ± 26 min, and 67 ± 14 min. It is worth noting that Figure 4a and Subject 1 of Figure 5a correspond to the same subject. The results from iontophoresis and exercise sweat show similar time of peak concentration (47 min versus 50 min). The sets of on-body studies are compared to the case where no fava beans are consumed, which demonstrates almost zero concentration of levodopa (Figure S4). The on-body experiments demonstrate the novelties and feasibilities of the wearable *s*-band for noninvasive and continuous monitoring of levodopa's dynamic metabolic rate. We envision that this sensor platform can enable clinical understanding of xenobiotic metabolisms and dosage optimizations.

In summary, we demonstrated the performance of a wearable sweat band for monitoring the metabolic behavior

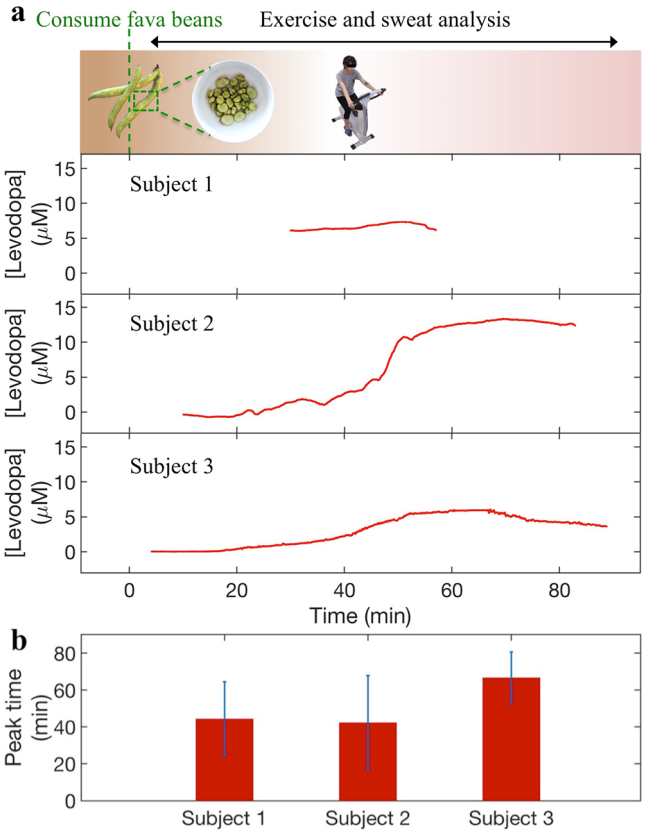

Figure 5. Levodopa monitoring via exercise induced sweat. (a) Cycling and sweat analysis. Examples of sweat levodopa concentrations for three different subjects after they consume 450 g of fava beans. (b) Averaged time of peak levodopa concentration for three different subjects across multiple exercise trials.

of levodopa, the standard medication prescribed to Parkinson's disease patients. The levodopa *s*-band integrates various material innovations and enables us to gain fundamental insights into the pharmacokinetic behavior of levodopa noninvasively. Dendritic growth, enzyme immobilization, and stabilizing film are seamlessly incorporated to improve the robustness and stability of the electrochemical sensor. We have also demonstrated the application of the *s*-band for prolonged, continuous, and noninvasive drug monitoring in human subjects after fava beans intake. Through analyzing sweat generated via iontophoresis and physical activities, the metabolism of the drug can be tracked in real-time to allow for dosage optimization. Future directions include investigating pharmacodynamics between drugs, lengthening iontophoresis sweating duration, and improving electrode lifetime upon repeated use. We envision that the wearable *s*-band can be leveraged to study the intrinsically complex drug profiles, optimize drug dosages to regulate Parkinsonian behaviors in patients, and integrate with drug delivery systems. This platform serves as a pathway toward drug management for increasingly personalized, point-of-care medicine for the future.

Methods. *Sensor Fabrication.* The flexible electrodes were fabricated on PET substrates via photolithography and evaporation. The electrodes were patterned through photolithography with positive photoresist (Shipley Microposit S1818) and electron-beam evaporation of Cr (30 nm) and Au (50 nm). Afterward, lift-off in acetone solution was performed. Au nanodendrites were grown on top of the

DOI: 10.1021/acs.nanolett.9b02478
Nano Lett. XXXX, XXX, XXX−XXX

electrodes with a Gamry Electrochemical Potentiostat (signal type, square wave; signal frequency, 50 Hz; amplitude, 1 V; DC offset, −1 V; cycles, 6000) and chloroauric acid solution (mixture of 50 mM $AuCl_3$ and 50 mM HCl). The precursor concentration will affect the morphology and length of the nanostructures, while increasing the deposition time will normally increase the length of the nanostructures.[42] The 6000 cycles (120 s) of Au deposition were chosen because the resulting functionalized electrode showed the largest current change upon the addition of 10 μM of levodopa, as shown in Figure S3. The electrodes were immediately cleaned with deionized water and left at room temperature for 2 h for drying. On top of the Au nanodendrites, 0.25 mM of thionin acetate salt (Sigma-Aldrich) was deposited electrochemically with CV (initial potential, −0.6 V; final potential, 0.1 V; scan rate, 0.1 V/s; segment, 40). The electrodes were then left at room temperature for 2 h. Subsequently, a mixture of enzyme and cross-linker solution was drop-casted on top of the electrodes (2.5 μL). The solution was prepared by mixing tyrosinase (Sigma-Aldrich. One mg) with 2% glutaraldehyde (Sigma-Aldrich. 0.866 μL) in PBS (66.6 μL). The electrodes were left at room temperature for 12 h. Finally, Nafion 117 (Sigma-Aldrich. One μL) was drop-casted on top of the electrodes, and the electrodes were left at room temperature for 2 h. For the reference electrodes, Ag/AgCl paste was painted on top of the Au electrodes and left at room temperature for 12 h.

Sensor Characterization and Calibration. The functionalized electrodes were characterized electrochemically using CHI 1230C potentiostat (CH Instrument) in CV and amperometric measurements. The CV and amperometric responses corresponding to different concentrations of levodopa were subsequently evaluated. The interference test involved the addition of various biomolecules at the physiologically relevant concentrations. In Figure 2, the functionalized working electrodes were characterized with commercial Ag/AgCl reference electrode in PBS. In Figure 3, on-body functionalized electrode arrays, including functionalized working electrodes, Ag/AgCl pasted reference electrodes, and Au counter electrodes (all on PET substrate), were characterized in sweat solutions collected from the exercise trials.

Iontophoresis Sweat Analysis. Iontophoresis was conducted by gently mounting pilocarpine hydrogel (ELITechGroup SS-023 Pilogel) on a subject's wrist for 5 min at 1 mA DC current (ELITechGroup Model 3700 Webster Sweat Inducer). During in situ evaluation, electrode arrays were placed conformal to the skin and connected to the CHI 1230C potentiostat. The on-body sweat analysis of human subjects was approved by the institutional review board (CPHS 2016−06−8853) at the University of California, Berkeley. The on-body sweat analyses were processed with MATLAB's Hampel and Smooth functions for noise reduction.

Exercise Sweat Analysis. The subjects engaged in stationary cycling on an ergometer (Gold's Gym 290C Upright Cycle Trainer) at a biking power of 100 W. The electrode arrays were calibrated and tested with the same method as that in the Iontophoresis Sweat Analysis section. The continuous data are plotted when the sensor starts to respond in sweat solutions. This corresponds to the time when we observe obvious sweating on the subject and sufficient accumulation of sweat around the sensor. The uncertainty for the time of peak concentration in Figure 5b was defined as the standard deviation of all the exercise trials for the same subject. One trial was performed for subject 3, and the uncertainty was estimated from the slope (concentration/time) around the proximity of the pharmacokinetic peak and the sensor drift (uncertainty in concentration).

Food Intake. Fava beans were purchased from a local community market (Berkeley Bowl). Two-hundred-fifty grams of fava beans consumption is equivalent to about 125 mg of levodopa intake.[18] The sandwich was a 12-in. Italian B. M. T. sandwich (Subway). The fava beans' seeds were taken out from the bean pods and cooked in boiling water for 20 min prior to consumption.

■ ASSOCIATED CONTENT

Supporting Information

The Supporting Information is available free of charge on the ACS Publications website at DOI: 10.1021/acs.nanolett.9b02478.

Method of determining peak potential; CV of levodopa dissolved in PBS tested with bare Au working electrode; long-term amperometric test for functionalized working electrode; levodopa sensor response with iontophoresis-induced sweat without fava beans consumption (PDF)

■ AUTHOR INFORMATION

Corresponding Author

*E-mail: ajavey@berkeley.edu.

ORCID

Li-Chia Tai: 0000-0001-7042-5109
Yuanjing Lin: 0000-0002-8568-1786
Hnin Y. Y. Nyein: 0000-0002-5692-6182
Mallika Bariya: 0000-0002-3416-8157
Wenbo Ji: 0000-0002-7913-361X
Zhiyong Fan: 0000-0002-5397-0129
Ali Javey: 0000-0001-7214-7931

Author Contributions

L.-C.T. and A.J. designed the experiments. L.-C.T., T.S.L., Y.L., and A.J. contributed to data collection, analysis, and interpretation. L.-C.T., T.S.L., Y.L., H.Y.Y.N., M.B., W.J., M.H., and C.Z. contributed to sensor fabrication and preparation. L.-C.T. and A.J. wrote the paper, and all authors provided feedback.

Notes

The authors declare no competing financial interest.

■ ACKNOWLEDGMENTS

This work was supported by the National Science Foundation (NSF) Nanomanufacturing Systems for Mobile Computing and Mobile Energy Technologies (NASCENT) and the Berkeley Sensor & Actuator Center (BSAC). The sensor fabrication was performed in the Electronic Materials (E-MAT) laboratory funded by the Director, Office of Science, Office of Basic Energy Sciences, Materials Sciences and Engineering Division of the U.S. Department of Energy under Contract No. DE-AC02-05CH11231.

■ REFERENCES

(1) Piccini, P.; Brooks, D. J.; Björklund, A.; Gunn, R. N.; Grasby, P. M.; Rimoldi, O.; Brundin, P.; Hagell, P.; Rehncrona, S.; Widner, H.; Lindvall, O. *Nat. Neurosci.* **1999**, *2*, 1137−1140.

DOI: 10.1021/acs.nanolett.9b02478
Nano Lett. XXXX, XXX, XXX−XXX

(2) Kravitz, A. V.; Freeze, B. S.; Parker, P. R. L.; Kay, K.; Thwin, M. T.; Deisseroth, K.; Kreitzer, A. C. *Nature* **2010**, *466*, 622−626.
(3) Garnett, E. S.; Firnau, G.; Nahmias, C. *Nature* **1983**, *305*, 137−138.
(4) Kortekaas, R.; Leenders, K. L.; van Oostrom, J. C. H.; Vaalburg, W.; Bart, J.; Willemsen, A. T. M.; Hendrikse, N. H. *Ann. Neurol.* **2005**, *57*, 176−179.
(5) van Kessel, S. P.; Frye, A. K.; El-Gendy, A. O.; Castejon, M.; Keshavarzian, A.; van Dijk, G.; El Aidy, S. *Nat. Commun.* **2019**, *10*, 310.
(6) Frankel, J. P.; Kempster, P. A.; Bovingdon, M.; Webster, R.; Lees, A. J.; Stern, G. M. *J. Neurol., Neurosurg. Psychiatry* **1989**, *52*, 1063−1067.
(7) Cotzias, G. C.; Van Woert, M. H.; Schiffer, L. M. N. *N. Engl. J. Med.* **1967**, *276*, 374−379.
(8) Deleu, D.; Jacob, P.; Chand, P.; Sarre, S.; Colwell, A. *Neurology* **2006**, *67*, 897−899.
(9) Haaxma, C. A.; Bloem, B. R.; Borm, G. F.; Oyen, W. J. G.; Leenders, K. L.; Eshuis, S.; Booij, J.; Dluzen, D. E.; Horstink, M. W. I. M. *J. Neurol., Neurosurg. Psychiatry* **2007**, *78*, 819−824.
(10) Sossi, V.; de la Fuente-Fernández, R.; Schulzer, M.; Adams, J.; Stoessl, J. *Brain* **2006**, *129*, 1050−1058.
(11) Crevoisier, C.; Zerr, P.; Calvi-Gries, F.; Nilsen, T. *Eur. J. Pharm. Biopharm.* **2003**, *55*, 71−76.
(12) Svenningsson, P.; Rosenblad, C.; af Edholm Arvidsson, K.; Wictorin, K.; Keywood, C.; Shankar, B.; Lowe, D. A.; Björklund, A.; Widner, H. *Brain* **2015**, *138*, 963−973.
(13) Bézard, E.; Ferry, S.; Mach, U.; Stark, H.; Leriche, L.; Boraud, T.; Gross, C.; Sokoloff, P. *Nat. Med.* **2003**, *9*, 762−767.
(14) Picconi, B.; Centonze, D.; Håkansson, K.; Bernardi, G.; Greengard, P.; Fisone, G.; Cenci, M. A.; Calabresi, P. *Nat. Neurosci.* **2003**, *6*, 501−506.
(15) Senek, M.; Aquilonius, S.-M.; Askmark, H.; Bergquist, F.; Constantinescu, R.; Ericsson, A.; Lycke, S.; Medvedev, A.; Memedi, M.; Ohlsson, F.; Spira, J.; Westin, J.; Nyholm, D. *Eur. J. Clin. Pharmacol.* **2017**, *73*, 563−571.
(16) Harder, S.; Baas, H.; Rietbrock, S. *Clin. Pharmacokinet.* **1995**, *29*, 243−256.
(17) Nyholm, D.; Lewander, T.; Gomes-Trolin, C.; Bäckström, T.; Panagiotidis, G.; Ehrnebo, M.; Nyström, C.; Aquilonius, S.-M. *Clin. Neuropharmacol.* **2012**, *35*, 111−117.
(18) Rabey, J. M.; Vered, Y.; Shabtai, H.; Graff, E.; Korczyn, A. D. *J. Neurol., Neurosurg. Psychiatry* **1992**, *55*, 725−727.
(19) Tsunoda, M.; Hirayama, M.; Tsuda, T.; Ohno, K. *Clin. Chim. Acta* **2015**, *442*, 52−55.
(20) Kovacs, E. M. R.; Stegen, J. H. C. H.; Brouns, F. *J. Appl. Physiol.* **1998**, *85*, 709−715.
(21) Birkett, D. J.; Miners, J. O. *Br. J. Clin. Pharmacol.* **1991**, *31*, 405−408.
(22) Kintz, P.; Henrich, A.; Cirimele, V.; Ludes, B. *J. Chromatogr., Biomed. Appl.* **1998**, *705*, 357−361.
(23) Movlaee, K.; Beitollahi, H.; Ganjali, M. R.; Norouzi, P. *Microchim. Acta* **2017**, *184*, 3281−3289.
(24) Yue, H. Y.; Zhang, H.; Huang, S.; Lin, X. Y.; Gao, X.; Chang, J.; Yao, L. H.; Guo, E. J. *Biosens. Bioelectron.* **2017**, *89*, 592−597.
(25) Thieme, D.; Rautenberg, C.; Grosse, J.; Schoenfelder, M. *Drug Test. Anal.* **2013**, *5*, 819−825.
(26) Cone, E. J.; Hillsgrove, M. J.; Jenkins, A. J.; Keenan, R. M.; Darwin, W. D. *J. Anal. Toxicol.* **1994**, *18*, 298−305.
(27) Koh, A.; Kang, D.; Xue, Y.; Lee, S.; Pielak, R. M.; Kim, J.; Hwang, T.; Min, S.; Banks, A.; Bastien, P.; Manco, M. C.; Wang, L.; Ammann, K. R.; Jang, K.-I.; Won, P.; Han, S.; Ghaffari, R.; Paik, U.; Slepian, M. J.; Balooch, G.; Huang, Y.; Rogers, J. A. *Sci. Transl. Med.* **2016**, *8*, 366ra165.
(28) Matzeu, G.; Fay, C.; Vaillant, A.; Coyle, S.; Diamond, D. *IEEE Trans. Biomed. Eng.* **2016**, *63*, 1672−1680.
(29) Tai, L.-C.; Gao, W.; Chao, M.; Bariya, M.; Ngo, Q. P.; Shahpar, Z.; Nyein, H. Y. Y.; Park, H.; Sun, J.; Jung, Y.; Wu, E.; Fahad, H. M.; Lien, D.-H.; Ota, H.; Cho, G.; Javey, A. *Adv. Mater.* **2018**, *30*, 1707442.
(30) Gao, W.; Emaminejad, S.; Nyein, H. Y. Y.; Challa, S.; Chen, K.; Peck, A.; Fahad, H. M.; Ota, H.; Shiraki, H.; Kiriya, D.; Lien, D.-H.; Brooks, G. A.; Davis, R. W.; Javey, A. *Nature* **2016**, *529*, 509−514.
(31) Emaminejad, S.; Gao, W.; Wu, E.; Davies, Z. A.; Nyein, H. Y. Y.; Challa, S.; Ryan, S. P.; Fahad, H. M.; Chen, K.; Shahpar, Z.; Talebi, S.; Milla, C.; Javey, A.; Davis, R. W. *Proc. Natl. Acad. Sci. U. S. A.* **2017**, *114*, 4625−4630.
(32) Kim, J.; Jeerapan, I.; Imani, S.; Cho, T. N.; Bandodkar, A.; Cinti, S.; Mercier, P. P.; Wang, J. *ACS Sens.* **2016**, *1*, 1011−1019.
(33) Krishnan, S. R.; Ray, T. R.; Ayer, A. B.; Ma, Y.; Gutruf, P.; Lee, K.; Lee, J. Y.; Wei, C.; Feng, X.; Ng, B.; Abecassis, Z. A.; Murthy, N.; Stankiewicz, I.; Freudman, J.; Stillman, J.; Kim, N.; Young, G.; Goudeseune, C.; Ciraldo, J.; Tate, M.; Huang, Y.; Potts, M.; Rogers, J. A. *Sci. Transl. Med.* **2018**, *10*, No. eaat8437.
(34) Takei, K.; Takahashi, T.; Ho, J. C.; Ko, H.; Gillies, A. G.; Leu, P. W.; Fearing, R. S.; Javey, A. *Nat. Mater.* **2010**, *9*, 821−826.
(35) Ota, H.; Chen, K.; Lin, Y.; Kiriya, D.; Shiraki, H.; Yu, Z.; Ha, T.-J.; Javey, A. *Nat. Commun.* **2014**, *5*, 5032.
(36) Boutry, C. M.; Beker, L.; Kaizawa, Y.; Vassos, C.; Tran, H.; Hinckley, A. C.; Pfattner, R.; Niu, S.; Li, J.; Claverie, J.; Wang, Z.; Chang, J.; Fox, P. M.; Bao, Z. *Nat. Biomed. Eng.* **2019**, *3*, 47−57.
(37) Brunetti, B.; Valdés-Ramírez, G.; Litvan, I.; Wang, J. *Electrochem. Commun.* **2014**, *48*, 28−31.
(38) Lin, Y.; Gao, Y.; Fan, Z. *Adv. Mater.* **2017**, *29*, 1701736.
(39) Wang, S.; Wu, Y.; Gu, Y.; Li, T.; Luo, H.; Li, L.-H.; Bai, Y.; Li, L.; Liu, L.; Cao, Y.; Ding, H.; Zhang, T. *Anal. Chem.* **2017**, *89*, 10224−10231.
(40) Dempsey, E.; Diamond, D.; Collier, A. *Biosens. Bioelectron.* **2004**, *20*, 367−377.
(41) Qi, L.; Thomas, E.; White, S. H.; Smith, S. K.; Lee, C. A.; Wilson, L. R.; Sombers, L. A. *Anal. Chem.* **2016**, *88*, 8129−8136.
(42) Ye, W.; Yan, J.; Ye, Q.; Zhou, F. *J. Phys. Chem. C* **2010**, *114*, 15617−15624.

DOI: 10.1021/acs.nanolett.9b02478
Nano Lett. XXXX, XXX, XXX−XXX